Aufhellung in series expansion solutions of three-beam X-ray diffractions

Sérgio L. Morelhão,[1,*] Luis H. Avanci,[1] and Stefan Kycia[2]

[1] *Instituto de Física, Universidade de São Paulo, CP 66318, 05315-970 SãoPaulo, SP, Brazil*
[2] *Laboratório Nacional de Luz Síncrotron/LNLS, CP 6192, 13084-971 Campinas, SP, Brazil*

(Dated: December 5, 2004)

Physical X-ray phase measurements are possible via *three*-beam diffraction experiments. Generalized and simple theoretical approaches have become a necessity for accessing this piece of information by means of practical and systematic procedures. Consistency of probabilities for the X-ray photons entering and leaving the crystal are exploited here to derive theoretical approaches accounting for *Aufhellung*, an energy balance effect among the simultaneously diffracted beams.

Keywords: X-ray diffraction, invariant phase determination, synchrotron radiation

I. INTRODUCTION

In the n-beam X-ray diffraction phenomenon, or multiwave diffraction, the reduction in the intensity of a *two*-beam diffraction owing to the excitement of other beams is known as *Aufhellung*.[1,2] It is directly related to the balance of energy among simultaneously diffracted beams.

For decades, the multiwave diffraction in single crystals has been extensively studied since it allows physical measurements of reflection phases, more precisely the invariant phase triplets.[2–5,13] The dynamical theory – the solution for the propagation of X-rays in crystals deduced from Maxwell's equations – describes all elementary concepts of crystal optics for X-rays, and also the n-beam diffraction. It provides the propagation modes of the electromagnetic fields in a perfect periodic infinite medium. Boundary conditions are required for determining the amplitudes of the diffracted waves in a finite crystal, which account for the energy balance among the diffracted beams. However, great efforts have also been dedicated in developing other theoretical approaches to embrace relevant aspects of the diffraction physics, such as crystalline imperfections, and to facilitate feasible analysis of experimental results.

The available approaches are limited solutions, mostly for *three*-beam diffraction cases, based on second-order[6–12,14] and third-order approximations derived either from Takagi-Taupin treatment[15–17] or from the fundamental equation of dynamical diffraction theory;[18] well-organized reviews on succeeding developments in this research field can be found in recent articles.[17,19] In most approaches, the diffracted intensities are given by

$$\mathrm{I_G} = \frac{c}{2\varepsilon_0}\left|\sum_{n=1}^{\mathrm{N}} \mathbf{D}_{n,\mathrm{G}}\right|^2 \qquad (1)$$

where the amplitude of the electric displacement field is written as a series expansion, and each term of the expansion, $\mathbf{D}_{n,\mathrm{G}}$, has its maximum contribution, in modulus, at the maximum of the *multi*-beam excitement condition.

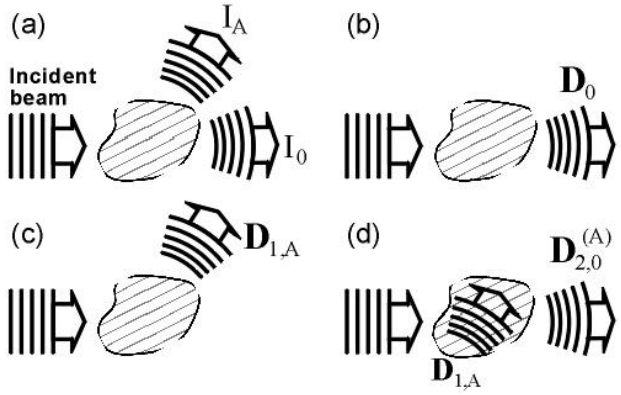

FIG. 1: X-ray scattering in a small crystal undergoing *two*-beam diffraction. (a) Measurable transmitted $\mathrm{I_0}$, and reflected $\mathrm{I_A}$, intensities; (b) forward-transmitted wave $\mathbf{D}_0$; (c) first-order reflected wave $\mathbf{D}_{1,\mathrm{A}}$, owing to the excitament of reflection A; and (d) second-order wave $\mathbf{D}_{2,0}^{(\mathrm{A})}$, generated by the rescattering of $\mathbf{D}_{1,\mathrm{A}}$ in the $\bar{\mathrm{A}}$ reflection.

A. Detailed description of the problem

The motivation of this work is the fact that it is not trivial to take *Aufhellung* into account by series expansion solutions of the fields as defined in Eq. (1); the inclusion of higher-order terms do not account for *Aufhellung* as suggested by several authors[18]. The reason is that

$$\left|\sum_{n=1}^{\mathrm{N}} \mathbf{D}_{n,\mathrm{G}}\right|^2 < \left|\sum_{n=1}^{\mathrm{N-1}} \mathbf{D}_{n,\mathrm{G}}\right|^2$$

occurs exclusively due to interference effects. Each additional term of the series expansion can reduce or enhance the diffracted intensity depending on its relative phase to the other terms. Individually, or in the absence of interference effects, each term represents some amount of energy contributing to the diffracted intensity, which is the opposite effect of *Aufhellung*.

The deficiency of series expansion form of solution to account for *Aufhellung* can be better demonstrated by means of an example. Let assume the small non-absorbing crystal in Fig. 1, where third-order terms as

well as higher order ones are negligible, i.e. $\mathbf{D}_{n\geq 3,\mathrm{G}} \approx 0$ for G = 0 or A. Then,

$$\mathtt{I}'_0 = \frac{c}{2\varepsilon_0}\left|\mathbf{D}'_0 + \mathbf{D}'^{(\mathrm{A})}_{2,0}\right|^2 \tag{2a}$$

and

$$\mathtt{I}'_\mathrm{A} = \frac{c}{2\varepsilon_0}\left|\mathbf{D}'_{1,\mathrm{A}}\right|^2 \tag{2b}$$

are the intensities under *two*-beam diffraction, as in Fig. 1(a). $\mathbf{D}'_0$ is the forward-transmitted wave Fig. 1(b), and $\mathbf{D}'_{1,\mathrm{A}}$ is the first-order reflected wave owing to the excitament of reflection A, Fig. 1(c). A second-order wave $\mathbf{D}'^{(\mathrm{A})}_{2,0}$, towards the forward-transmitted one is generated by the propagation of $\mathbf{D}'_{1,\mathrm{A}}$ inside the crystal under diffraction condition for the $\bar{\mathrm{A}}$ reflection, Fig. 1(d).

When another reflection is simultaneously excited, for instance reflection B, the diffracted intensities become

$$\mathtt{I}_0 = \frac{c}{2\varepsilon_0}\left|\mathbf{D}_0 + \mathbf{D}^{(\mathrm{A})}_{2,0} + \mathbf{D}^{(\mathrm{B})}_{2,0}\right|^2, \tag{3a}$$

$$\mathtt{I}_\mathrm{A} = \frac{c}{2\varepsilon_0}\left|\mathbf{D}_{1,\mathrm{A}} + \mathbf{D}^{(\mathrm{B})}_{2,\mathrm{A}}\right|^2, \tag{3b}$$

and

$$\mathtt{I}_\mathrm{B} = \frac{c}{2\varepsilon_0}\left|\mathbf{D}_{1,\mathrm{B}} + \mathbf{D}^{(\mathrm{A})}_{2,\mathrm{B}}\right|^2 . \tag{3c}$$

(A,B) superscripts are used on the second-order waves to identify the first-order ones originating them.

Since the incident beam is constant in time, the total intensity of the diffracted waves under *two*-beam and *three*-beam diffraction conditions are equal, i.e. $\mathtt{I}'_0+\mathtt{I}'_\mathrm{A} = \mathtt{I}_0 + \mathtt{I}_\mathrm{A} + \mathtt{I}_\mathrm{B}$ or

$$\left|\mathbf{D}'_0 + \mathbf{D}'^{(\mathrm{A})}_{2,0}\right|^2 + \left|\mathbf{D}'_{1,\mathrm{A}}\right|^2 = \left|\mathbf{D}_0 + \mathbf{D}^{(\mathrm{A})}_{2,0} + \mathbf{D}^{(\mathrm{B})}_{2,0}\right|^2 + \left|\mathbf{D}_{1,\mathrm{A}} + \mathbf{D}^{(\mathrm{B})}_{2,\mathrm{A}}\right|^2 + \left|\mathbf{D}_{1,\mathrm{B}} + \mathbf{D}^{(\mathrm{A})}_{2,\mathrm{B}}\right|^2 . \tag{4}$$

There are two major difficults in series expansion solutions: *i)* the convergence properties of the series under *multi*-beam diffraction regime, which is the time-independent solution, or the solution for the crystal in a fixed position; and *ii)* the time-dependent solution capable to describe the selective excitament of the beams until the *multi*-beam configuration is achieved. It can be summarized in the above example, in how to go from Eqs. (2) to Eqs. (3) without violating the equality in Eq. (4). In more specific words, it is necessary to describe not only how the extra terms in Eqs. (3) are excited, but also how the terms already excited in Eqs. (2) are affected by the excitement of another beam, which is $\mathtt{I}_\mathrm{B}$ in this example. For a qualitative description, one may assume that $\mathbf{D}_0 = \mathbf{D}'_0$, $\mathbf{D}^{(\mathrm{A})}_{2,0} = \mathbf{D}'^{(\mathrm{A})}_{2,0}$, and $\mathbf{D}_{1,\mathrm{A}} = \mathbf{D}'_{1,\mathrm{A}}$, and that the extra terms in Eqs. (3) are switched-on as the crystal rotates to excite $\mathtt{I}_\mathrm{B}$. However, in this description the total diffracted intensity is not preserved, and that ends any possibility to correctly account for *Aufhellung*.

Nevertheless, such qualitative description provides good results for particular cases where $\mathbf{D}^{(\mathrm{B})}_{2,0}$ and $\mathbf{D}^{(\mathrm{B})}_{2,\mathrm{A}}$ have destructive interferences with the other terms of $\mathtt{I}_0$ and $\mathtt{I}_\mathrm{A}$ in Eqs. (3a) and (3b), respectively; and these destructive interferences account for some amount of the intensity transfered to $\mathtt{I}_\mathrm{B}$. Although some phase relationships may exist among the diffracted waves, they vary from one crystal to another since the structure factor phases are intrinsically related to the internal three-dimensional structure of the crystals. Therefore, for a general solution, the balance of energy among simultaneously diffracted beams should not rely on phase relationships among terms of the series expansions.

To account for *Aufhellung*, it is proposed a treatment of the *multi*-beam diffraction phenomenon based on preservation of classical probabilities for X-ray photons entering and leaving the crystal. Emphasis is to the balance of energy, which appears naturally in this treatment. It allows convergent solutions even in cases where *Aufhellung* can not be neglected, as experimentally demonstrated for *three*-beam diffraction cases. Interference of probability amplitudes for photons is included to take phase sensitivity into account, and to provide mechanisms to correctly estimate the contributions of higher order terms in the solution of the diffracted intensities. Moreover, the demonstrative experimental dataset also carries some information on chemical bounding-charges, as shortly discussed.

II. GENERAL SOLUTION

Classical and quantum concepts of probability have been recently applied to describe the *two*-beam diffraction in reflection geometry.[20] By following the classical trajectories of X-ray photons inside a periodic lattice and preserving their probabilities for reflection, transmission and absorption at each lattice plane, classical scattering outcomes are obtained. Diffraction phenomena in crystals were reproduced after assigning quantum probability amplitudes[21] to every classical outcome.

Under *multi*-beam diffraction, the classical outcomes are obtained by visualizing the photons as classical particles; in this context, X-ray beams "...are streams of globules, like bullets from a machine gun". It allows the definition of $p_{G,H}(n)$ as the X-ray photon diffraction probability from beam H to beam G after n diffraction events (bounces) inside the crystal. The population $P_G(n)$ of n-bounced photons in the beam G is then calculated as

$$P_G(n+1) = \sum_{H \neq G} p_{G,H}(n) P_H(n) \, . \tag{5}$$

$P_0(0) = N_0$ stands for the incident number of photons per unit of time, and the time-dependence of the $p_{G,H}(n)$ probabilities are determined by the crystal rotation, i.e. on how the crystal position varies in time until the -beam configuration is achieved.

Assuming a slow time variation to assure that at any time instant the populations are given by Eq. (5), their behaviors as a function of n can be infered by the sum of diffraction probabilites,

$$s_G(n) = \sum_{H \neq G} p_{H,G}(n) \, . \tag{6}$$

These values are interconnected by consistency of probabilities to exiting probabilites defined as

$$d_G(n) = 1 - a_G(n) - s_G(n) \tag{7}$$

where $a_G(n)$ is the probability of the photons in the beam G to be absorbed after n bounces. Since $d_G(n)$ is the fraction of n-bounced photons that will effectively leave the crystal via beam G, the diffracted intensities (in number of photons per unit of time) outside the crystal are given by

$$I_{G[N]} = \sum_{n=1}^{N} d_G(n) P_G(n) \, . \tag{8}$$

For $N_0 = 1$, $d_G(n)P_G(n)$ corresponds to the total probability of the incident photon to interact and to leave the crystal via one of the n-bounce channels ending on beam G. – each channel is a different sequence of reflections inside the crystal. – It garantees the balance of energy among the diffracted beams since

$$\lim_{N \to \infty} \sum_{G} I_{G[N]} = N_0 \, , \tag{9}$$

and hence, the converge of the series expansion in Eq. (8).

However, X-ray photons are quantum particles and, consequently, the diffracted intensities also depend on interference effects among the probability amplitudes of the different diffraction channels. To explicitaly shown this dependence it is necessary to replace the sum of probabilities by the square modulus of the sum of probability amplitudes, which are related to the amplitudes of the electric displacement fields. It leads to

$$I_{G[N]} = K \left| \sum_{n=1}^{N} \mathbf{D}_{n,G} \right|^2 \tag{10}$$

where each term stands for the total diffraction probability amplitude of all n-bounce channels ending on beam G since

$$K |\mathbf{D}_{n,G}|^2 = d_G(n) P_G(n). \tag{11}$$

K converts wavefield square units to number of photons per unit of time diffracted within a given solid angle.

The physical meaning of $d_G(n)$ is to reduce, according to Eq. (7), the probability amplitude of diffraction towards beam G when other beams are excited, i.e. when the photons on beam G, inside the crystal, have a non null probability of leaving the crystal via other beams. Therefore, the series expansion terms of this solution do not necessarily have their maximum amplitude, in modulus, at the maximum of the *multi*-beam condition as found in previous approaches, e.g. in Eq. (1).

The classical treatment of the photon populations, Eqs. (5) through (8), can provide only the square modulii of the amplitudes in Eq. (10). It has still to be improved to account for the phases of the diffracted waves, as well as for the time-dependence of the $p_{G,H}(n)$ probabilities.

Limited to *three*-beam diffraction cases (3BD), the phases of the diffracted waves up to the third-order approximation are already available in the literature.[16,18] For this reason, the present developtments and discussions will be henceforth limited to 3BD cases.

III. THREE-BEAM X-RAY DIFFRACTION

A general 3BD configuration is schematically illustrated in Fig. 2(a). For sake of simplicity, the $p_{G,H}$ diffraction probabilities are rewritten as r_X where X (= A, B, C, $\bar{A}$, $\bar{B}$, or $\bar{C}$) indicates the Bragg reflection transfering energy from beam H to beam G. Using these probabilities in Eq. (5), the photon populations on the three diffracted beams G = 0, A, and B, are

$$\begin{aligned} P_0(n+1) &= r_{\bar{A}} P_A(n) + r_{\bar{B}} P_B(n) \\ P_A(n+1) &= r_A P_0(n) + r_C P_B(n) \\ P_B(n+1) &= r_B P_0(n) + r_{\bar{C}} P_A(n) \, . \end{aligned} \tag{12}$$

The classical trajectories of the photons inside the crystal are represented at the diagram in Fig. 2(b); by following its loops or exiting at the bottom of each column all

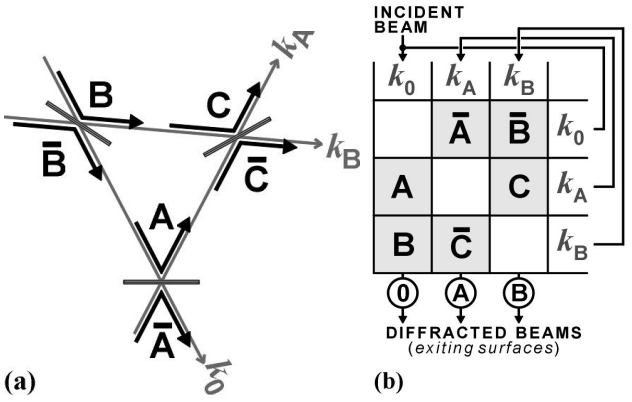

FIG. 2: X-ray *three*-beam diffraction in crystals: (a) planar scheme of the involved A, B, C, $\bar{A}$, $\bar{B}$, and $\bar{C}$ reflections and $\boldsymbol{k}_0$, $\boldsymbol{k}_A$, and $\boldsymbol{k}_B$ wavevectors; (b) diagram of probabilities where each column represents the diffraction, r_X (boxes), exiting, d_G (circles), and absorption, a_G, probabilities for X-ray photons in the beam G (= 0, A, and B). The sum of these probabilities at each column must be equal to 1. For instance, in the incident beam column (first column at left), a forward-transmited beam of non-diffracted photons occurs only when $d_0 = 1 - a_0 - r_A - r_B > 0$. All possible diffraction channels can be identified by following the loops of this diagrama, but in general the r_X, d_G, and a_G probabilities are dynamical variables changing at each loop.

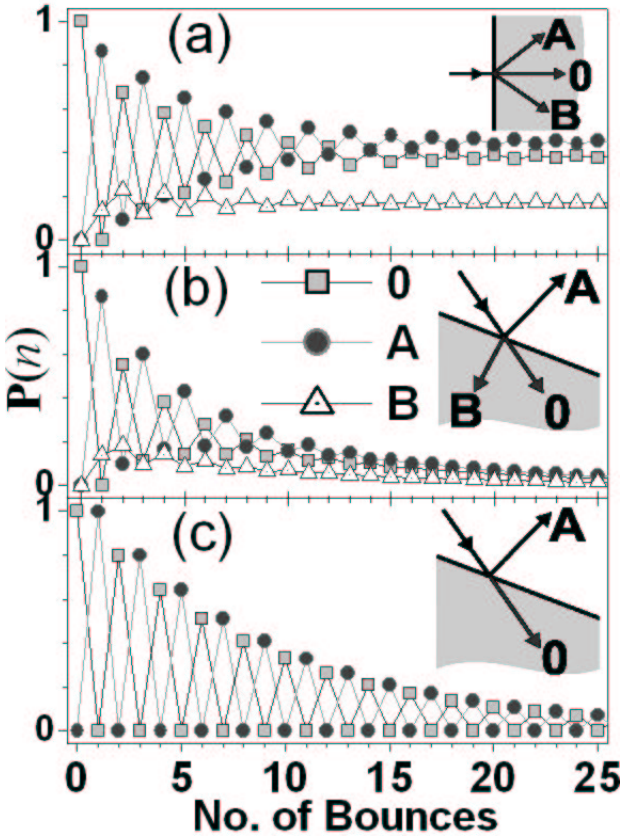

FIG. 3: Populations of n-bounced photons, P(n) [Eq. (12)], in the diffracted beams inside a semi-infinity crystal, calculated for $R_A = R_{\bar{A}}$, $R_B = R_{\bar{B}} = 0.16R_A$, and $R_C = R_{\bar{C}} = 0.36R_A$ where R_X is the intensity reflectivity of reflection X under 3-BD condition. (a) Laue-Laue case ($s_G = 1$): [r_A r_B $r_{\bar{A}}$ $r_{\bar{C}}$ $r_{\bar{B}}$ r_C] = [0.862 0.138 0.735 0.265 0.308 0.692]; (b) Bragg-Laue case ($s_A = 0.8$): [0.862 0.138 0.588 0.212 0.308 0.692]; and (c) Bragg *two*-beam case ($s_A = 0.8$, $R_B = R_{\bar{C}} = 0$): [1.0 0.0 0.8 0.0 0.0 0.0]. The r_X probabilities were obtained as $r_{A,B} = s_0 R_{A,B}/(R_A + R_B)$, $r_{\bar{A},\bar{C}} = s_A R_{\bar{A},\bar{C}}/(R_{\bar{A}} + R_{\bar{C}})$, and $r_{\bar{B},C} = s_B R_{\bar{B},C}/(R_{\bar{B}} + R_C)$.

possible diffraction channels are determined. At each column of the diagram, diffraction, exiting, and absorption probabilities are preserved. For instance, the incident photons (first column at left) have the r_A and r_B probabilities of diffraction toward beams A and B, respectively. If $r_A + r_B = 1$ all incident photons will be diffracted toward one of these beams, otherwise, $d_0 + a_0 = 1 - r_A - r_B$ provides the probability of the photons to leave the crystal via the incident beam direction plus their probability of absorption. More insights on the intrinsic correlation among diffraction and exiting probabilities can be achieved by discussing a few examples.

A. Diffraction geometry and exiting probabilities

In Laue-Laue diffraction geometry there are three diffracted-'transmitted' beams, as illustrated in the inset of Fig. 3(a). A non-absorbing semi-infinity crystal in this geometry is represented by $s_G = 1$, and hence $a_G = d_G = 0$. Since $r_A + r_B = 1$, $r_{\bar{A}} + r_{\bar{C}} = 1$, and $r_{\bar{B}} + r_C = 1$ the photons are bouncing endlessly from one beam to another, and the photon populations tend to constant non-null values, as shown in Fig. 3(a). No diffracted beams are measured outside the crystal, $I_G = 0$, since the photons will never reach the exiting surface at infinity. On the other hand, for a finite crystal slab there would be a minimum number of bounces, n_L, necessary for the photons to reach the exiting surface. For $n < n_L$ the exiting probabilities are zero, i.e. $d_G \approx 0$, and the behavior of the populations are very similar to that shown in Fig. 3(a); but, for $n > n_L$ the populations vanish and diffracted beams are measurables as $I_G \approx P_G(n_L)$ since $d_G(n_L) \approx 1$ in Eq. (8).

A different situation occurs when absorption or exiting probabilities are not null, and hence $s_G < 1$. In this case, all populations decrease as a function of n, as for instance depicted in Fig. 3(b) where the only difference with respect to Fig. 3(a) is that $s_A = 0.8$, or $d_A + a_A = 0.2$. If $d_A = 0$ the decrease of the populations is owing to absorption only, and the diffracted intensities are still zero. However, for $0 < d_A < 0.2$ some photons on beam A can reach an exiting surface and then $I_A > 0$. In a semi-infinite crystal (of infinity thickness), it means that the beam A must be a Bragg-reflected beam; a Bragg-Laue diffraction geometry as illustrated in the inset of Fig. 3(b). A Bragg-Bragg diffraction geometry would

require $d_A > 0$ and $d_B > 0$.

Away from the 3BD condition, when only reflection A is excited, there is a total alternation in of the population numbers from one beam to the other, as observed in Fig. 3(c). In this particular example, all photons in the beam 0 are bounced towards beam A, and 80% of the photons in beam A are bounced back to beam 0. The general behavior is that all photons in P_A and P_0 have suffered, respectively, odd ($n = 1, 3, \cdot$) and even ($n = 0, 2, \cdot$) number of bounces.

It is very convenient to take exiting and diffraction probabilities as constant values instead of functions of n. These values are dynamical variables changing at each bounce owing either to the relative positioning of the exiting surfaces and polarization factors. In principle, it is possible to calculate the diffraction probabilities per length unit and to compute the polarization factors for each sequence of reflections. However, before upgrading the proposed approach to more realistic cases and to include interference effects according to Eq. (10), it is necessary to demonstrated that Eq. (8) is a time-dependent solution capable to describe the excitament of beams without violating the equality in Eq. (9), and hence capable to account for *Aufhellung*.

B. Time-dependent solutions

A time-dependent solution requires the preservation of the sum of probabilities in Eq. (7) as one or more diffraction probabilities change in time owing to the crystal's rotation. The first effect to be analysed is the splitting of energy between two reflections simultaneously diffracting a given beam, as for instance A and B, $\bar{A}$ and $\bar{C}$, or $\bar{B}$ and C reflections in Fig. 2(a).The analysis is carried out for the A and B reflections, and extended by analogy to the other two pairs of reflections.

For this demonstration, let assume a very small non-absorbing crystal where R_X gives the fraction of reflected photons by each individual reflection. When only reflection A is excited, the diffracted intensities according to Eq. (8) are

$$\mathtt{I}_{0[0]} = \mathtt{I}_0 = \mathtt{d}_0 \mathtt{P}_0(0) = (1 - r_A)\mathtt{N}_0$$

and

$$\mathtt{I}_{A[1]} = \mathtt{I}_A = \mathtt{d}_A \mathtt{P}_A(1) = r_A \mathtt{N}_0$$

where $d_0 = 1 - r_A$, $r_A = R_A$, and $d_A = 1$.

The problem in describing the excitement of reflection B, when A is already excited, is that $d_0 + r_A + r_B > 1$ since $d_0 + r_A = 1$. It implies that the previous exiting and diffraction probabilities, d_0 and r_A, must decrease as reflection B is switched-on. But, by how much should each one of these probabilities decrease? It seems complicated because reflections A and B are simultaneous events; otherwise, the diffracted intensities could be calculated as shown in Fig. 4. If the diffraction probabilities

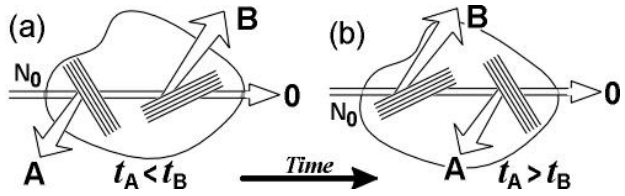

FIG. 4: Simultaneousness of diffraction events and their effects on the diffracted intensities. (a) Reflection A occurs before reflection B: $\mathtt{I}_A = R_A \mathtt{N}_0$, $\mathtt{I}_B = R_B(1 - R_A)\mathtt{N}_0$, and $\mathtt{I}_0 = (1 - R_B)(1 - R_A)\mathtt{N}_0$. (b) Reflection B occurs before reflection A: $\mathtt{I}_B = R_B \mathtt{N}_0$, $\mathtt{I}_A = R_A(1 - R_B)\mathtt{N}_0$, and $\mathtt{I}_0 = (1 - R_A)(1 - R_B)\mathtt{N}_0$. For time coincidental reflections, the outcome is the average of (a) and (b): $\mathtt{I}_A = R_A(1 - 0.5R_B)\mathtt{N}_0$ and $\mathtt{I}_B = R_B(1 - 0.5R_A)\mathtt{N}_0$.

are taken from the average values between the two hypothetical situations in Figs. 4(a) and 4(b), we have

$$r_A = R_A(1 - \tfrac{1}{2}R_B), \tag{13a}$$

$$r_B = R_B(1 - \tfrac{1}{2}R_A), \tag{13b}$$

and

$$s_0 = r_A + r_B = R_A + R_B - R_A R_B\,. \tag{13c}$$

These equations have simmetry with respect to the excitament of one reflection, B or A, when the other, A or B, is already excited. Therefore, the decrease in r_A, or r_B, owing to the excitament of reflection B, or A, is given by Eq. (13a), or Eq. (13b), respectively. The decrease in $d_0 = 1 - s_0$ is given by Eq. (13c). When absorption is taken into account, $d_0 = 1 - a_0 - s_0$ and the maximum value of s_0 is limited in the range from 0 to 1-a_0.

In large crystals the above solution fails. For instance, a non-divergent incident beam undergoes total reflection for both reflection, i.e. $R_A \simeq R_B \simeq 1$, and therefore $r_A \simeq r_B \simeq \frac{1}{2}$, which is not truth. The values of r_A and r_B should depend on the ratio between the square modulii of the structure factors. To extend the energy splitting solution in Eqs. (13) to crystal of medium size, where the series expansion of the fields only require a few terms, the crystal's dimension ℓ_G, along a given beam direction is divided into m identical layers of thickness $\Delta\ell$, with known reflectivities $\mathcal{R}_X$, and absorption probabilities a_G. The total diffraction probabilities are then obtained as the sum over m. For the beam 0, it provides

$$\begin{bmatrix} r_A \\ r_B \end{bmatrix} = \frac{1 - d_0}{s_0 + a_0} \begin{bmatrix} \mathcal{R}_A(1 - \frac{1}{2}\mathcal{R}_B) \\ \mathcal{R}_B(1 - \frac{1}{2}\mathcal{R}_A) \end{bmatrix} \tag{14}$$

In the limit of very thin layers $\mathcal{R}_X \ll 1$, the products of reflectivities such as $\mathcal{R}_A\mathcal{R}_B$ can be disregarded, so that $s_0 \simeq \mathcal{R}_A + \mathcal{R}_B$ and $d_0 = (1 - s_0 - a_0)^m \simeq \exp[-m(s_0 + a_0)]$.

The differences between Eqs. (13) and (14) become more significant as $m \to \infty$ since for $m = 1$ their results

are identicals. For an infinity non-absorbing crystal along the indident beam, i.e. $\ell_0 \to \infty$ and $a_0 = 0$, $r_{\rm A,B} = \tilde{\mathcal{R}}_{\rm A,B}$ where $\tilde{\mathcal{R}}_{\rm A,B} = \mathcal{R}_{\rm A,B}/s_0$. It provides different results for $r_{\rm A}$ and $r_{\rm B}$ since $\mathcal{R}_{\rm X}$ is the kinematical reflectivity of very thin layers, proportional to the structure factor square modulus. When absorption is allowed, $d_0 \to 0$ independently of the A and B reflections, and $a_0 = a_0/(s_0 + a_0)$ is the fraction of absorbed photons so that $r_{\rm A} + r_{\rm B} + a_0 = 1$.

Linear diffraction and absorption coefficients, corresponding to diffraction and absorption probabilities per unit length along each beam direction, can be defined as

$$\mu = \frac{a_{\rm G}}{\Delta\ell} \quad \text{and} \quad \mu_{\rm G} = \frac{s_{\rm G}}{\Delta\ell} \tag{15}$$

where μ is the linear absorption coefficient of the material. It allows the diffraction probabilities in Eq. (14), as well as the other ones, to be written as

$$\begin{bmatrix} r_{\rm X} \\ r_{\rm Y} \end{bmatrix} = \frac{1 - d_{\rm G}}{1 + \mu/\mu_{\rm G}} \begin{bmatrix} \tilde{\mathcal{R}}_{\rm X} \\ \tilde{\mathcal{R}}_{\rm Y} \end{bmatrix} \tag{16}$$

X and Y stands for the pair of reflections simultaneously diffracting the beam G, and

$$d_{\rm G} = e^{-(\mu+\mu_{\rm G})\ell_{\rm G}} \tag{17}$$

is the effective exiting probability through beam G.

In practice, knowledge on μ and $d_{\rm G}(n)$ values are required for a description of the diffraction process where the condition imposed by Eq. (9) is always satisfied as a function of the crystal rotation. Since $\Delta\ell$ can be as small as the lattice plane distances, $R_{\rm X}$ can be taken by the photon reflection probability[20] when crossing a single lattice plane. It is a very small number, of the order of 10^{-9} to 10^{-7} in crystals such as silicon and germanium. The contribution of reflection X to the linear diffraction coefficient, $\mu_{\rm G} = \mu_x + \mu_y$ in Eq. (15), is given by

$$\mu_x = \frac{R_{\rm X}}{\Delta\ell = d} = \frac{1}{d}\left(\frac{r_e\lambda|C||F_{\rm X}|d}{V_c \sin\theta}\right)^2 \tag{18}$$

where θ and d are the Bragg angle and lattice plane distance of the reflection X, respectively. V_c is the unit cell volume, $r_e = 2.818 \times 10^{-5}$Å the classical electron radius, and λ is the X-ray wavelength. For linearly polarized X-rays, the polarization factor

$$|C| = |\hat{\boldsymbol{k}}_{\rm H} \times (\hat{\boldsymbol{v}}_{n,G} \times \hat{\boldsymbol{k}}_{\rm H})|^2 \tag{19}$$

depends on polarizatin direction $\hat{\boldsymbol{v}}_{n,G}$, of the photons on beam G after n bounces, and on the direction of the diffracted beam H given by $\boldsymbol{k}_{\rm H} = \boldsymbol{X} + \boldsymbol{k}_{\rm G}$; $\boldsymbol{X}$ is the diffraction vector of reflection X.

Since elastic scatterings are the only contribution to reflection probabilities[20], the structure factors are calculated as

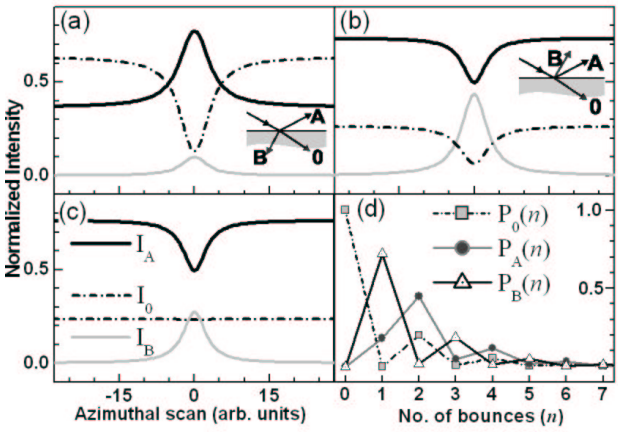

FIG. 5: Intensity variation in *two*-beam diffraction cases, I_0 and $\mathrm{I}_{\rm A}$, owing to the excitament of the secondary reflection B by the ϕ rotation (azimuthal scan) of the crystal around the diffraction vector of the primary reflection A, Eq. (22). The intensities are calculated by Eq. (8) for the following cases: (a) Bragg-Laue case with the parameter vector $\boldsymbol{p} = [|F_{\rm A}|\ |F_{\rm B}|\ |F_{\rm C}|\ \mathrm{d}_0\ \mathrm{d}_{\rm A}\ \mathrm{d}_{\rm B}]$=[2 4 6 0.1 0.9 0.1]; (b) Bragg-Bragg case: $\boldsymbol{p}$ = [4 4 0 0.05 0.8 0.7] in the same scale of (a); and (c) $\boldsymbol{p}$ = [4 0 6 0.2 0.5 0.8]. (d) Photon populations as a function of the number of bounces n for the 3BD case in (c). The $\boldsymbol{p}$ values are used in §III.B. to calculate the diffraction probabilities $r_{\rm X}$, at the maximum of the 3BD, but for sake of simplicity in this demonstration $\mu_x = \kappa|F_{\rm X}|^2$ in Eq. (18) where $\kappa \ll 1$. Since $\mu = 0$, $\mathrm{I}_0 + \mathrm{I}_{\rm A} + \mathrm{I}_{\rm B} = \mathrm{N}_0 = 1$.

$$F_{\rm X} = \sum_a (f + f')_a \exp(2\pi i \boldsymbol{X} \cdot \boldsymbol{r}_a) = |F_{\rm X}| e^{i\delta_X}, \tag{20}$$

which implies that $|F_{\rm X}| = |F_{\bar{\rm X}}|$ and $\delta_X + \delta_{\bar{X}} = 0$. a runs over all atoms in the unit cell. f and f' stand for the atomic scattering factor and its correction for atomic resonances, respectively. The linear absorption coefficient of the material is determined by the f'' correction of f, which provides

$$\mu = \frac{2\pi}{\lambda}\Gamma \sum_a f''_a \tag{21}$$

where $\Gamma = r_e\lambda^2/\pi V_c$.

C. *Aufhellung*

Occurrence of *Aufhellung* as a direct consequence of energy balance mechanisms is demonstrated for a few hypothetical cases in Fig. (5). The $d_{\rm G}(n)$ are taken by constant values as a function of n. It can be a good approximation when the population of photons become negligible just after a few bounces, e.g. Fig. 5(d).

Azimuthal rotation of the crystal around the diffraction vector of a given reflection, for instance reflection A,

is a systematic procedure to achieve the 3BD configuration in Fig. 2(a). The effects of the ϕ rotation on the diffracted intensities are taken into account by replacing

$$R_{\mathrm{B},\bar{\mathrm{C}}} \rightarrow R_{\mathrm{B},\bar{\mathrm{C}}}(\phi) = R_{\mathrm{B},\bar{\mathrm{C}}} L(\Delta\phi) \tag{22}$$

in Eqs. (16) and (18). $L(\Delta\phi)$ is a lorentzian function of unit weight, $L(\Delta\phi = 0) = 1$. $\Delta\phi = \phi - \phi_0$ stands for the deviation in the rotation angle ϕ, from the 3BD condition at ϕ_0.

As the crystal rotates, the intensities $\mathtt{I}_0$ and $\mathtt{I}_\mathrm{A}$ of the *two*-beam cases are balanced with the third beam intensity $\mathtt{I}_\mathrm{B}$. How the intensities change depends on the relative strengh of the involved reflections, as well as on the exiting probabilities d_G. But, in all cases and at any instant,

$$\mathtt{I}_0 + \mathtt{I}_\mathrm{A} + \mathtt{I}_\mathrm{B} = \mathrm{N}_0$$

since $\mu = 0$ for the cases in Fig. (5). Intensity reduction, named *Aufhellung*,[1] on the primary beam A can be observed in Figs. 5(b) and 5(c), while intensity enhancement, *Umweganregung*,[22] is observed in Fig. 5(a).

D. Amplitude and interference of diffracted fields

In the third-order solution of the primary beam intensity $\mathtt{I}_{\mathrm{A}[3]}$, Eq. (10), there are 5 channels contributing to the diffracted fields. They can be identified by following the loops in Fig. 2(b):

–Channel A

$$K|\mathbf{D}_{1,\mathrm{A}}|^2 = \mathrm{d}_\mathrm{A}(1)\mathrm{P}_\mathrm{G}(1) = d_\mathrm{A} r_\mathrm{A} = |\boldsymbol{D}_A|^2 \tag{23a}$$

–Channel BC

$$K|\mathbf{D}_{2,\mathrm{A}}|^2 = \mathrm{d}_\mathrm{A}(2)\mathrm{P}_\mathrm{G}(2) = d_\mathrm{A} r_\mathrm{A} r_\mathrm{B} = |\boldsymbol{D}_{BC}|^2 \,; \tag{23b}$$

–Channels AAA, BBA, and ACC

$$\begin{aligned} K|\mathbf{D}_{3,\mathrm{A}}|^2 &= \mathrm{d}_\mathrm{A}(3)\mathrm{P}_\mathrm{G}(3) \\ &= d_\mathrm{A}(r_\mathrm{A} r_{\bar{\mathrm{A}}} r_\mathrm{A} + r_\mathrm{B} r_{\bar{\mathrm{B}}} r_\mathrm{A} + r_\mathrm{A} r_{\bar{\mathrm{C}}} r_\mathrm{C}) \\ &= |\boldsymbol{D}_{AAA}|^2 + |\boldsymbol{D}_{BBA}|^2 + |\boldsymbol{D}_{ACC}|^2 \,. \end{aligned} \tag{23c}$$

The classical diffraction probability of each channel provides the square modulus of its probability amplitude.

Vectorial amplitudes and phases of the diffracted fields can be written as a 5×3 matrix (5 vectors, 3 components each)

$$[\mathcal{D}_{\alpha j}] = \begin{bmatrix} |\boldsymbol{D}_A|\, \hat{\boldsymbol{v}}_A \\ |\boldsymbol{D}_{BC}|\, e^{i(\Omega+\Psi)}\, \hat{\boldsymbol{v}}_{BC} \\ |\boldsymbol{D}_{AAA}|\, \hat{\boldsymbol{v}}_{AAA} \\ |\boldsymbol{D}_{BBA}|\, e^{i\Omega}\, \hat{\boldsymbol{v}}_{BBA} \\ |\boldsymbol{D}_{ACC}|\, e^{i\Omega}\, \hat{\boldsymbol{v}}_{ACC} \end{bmatrix} \tag{24}$$

where $\Psi = \delta_B + \delta_C - \delta_A$ is the invariant phase triplet, and $\hat{\boldsymbol{v}}_{channel}$ is the oscilation direction of each diffracted field determined by the polarization factors in Appendix A. $\Omega = \Omega(\phi)$ is the dynamical phase shift of the secondary waves.[4,12] If the resonant term[29] of the secondary reflection B is given by

$$\mathtt{f}(\phi) = \frac{w_s}{2(\phi - \phi_0) - i w_s} = |\mathtt{f}(\phi)| e^{i\Omega(\phi)} \,, \tag{25}$$

$L(\Delta\phi) = |\mathtt{f}(\phi)|^2$ in Eq. (22). $w_s = +w$ or $-w$ for *'out-in'* and *'in-out'* position, respectively; w is the FWHM of $|\mathtt{f}(\phi)|^2$.

This chosen $\mathtt{f}(\phi)$ function is similar to other functions already available in the literature,[16,18] and that have also been used to represent the ressonant term in third-order solutions of the primary field. Our preference by the specific function given in Eq. (25) resides on its simplicity and adjustable width.

The minimum value of w, which is w_{min}, corresponds to intrinsic width of the reflection curve (in reflection geometry), also known as the Darwin width. The rotation of the crystal around the ϕ-axis (parallel to the diffraction vector $\boldsymbol{A}$), instead of around an axis perpendicular to the incidence plane of reflection B, causes that, in general, $w > w_{min}$. Moreover, the intrinsic width also depends on polarization factors[30,31] and, as recently demonstrated,[20] can be calculated as a function of the photon reflection probability, R_X in Eq. (18), which provides

$$w_{min} \simeq \tfrac{2}{3}\sqrt{R_\mathrm{B}}\, \tan\theta_B. \tag{26}$$

The angular dependence of the diffracted fields in Eqs. (23) only accounts for the azimuthal rotation of the crystal. It implies that, according to the field definition in Eqs. (23), the primary intensity $\mathtt{I}_{\mathrm{A}[3]}(\phi)$ corresponds to the integrated photon counting rate in the rocking curve of the primary reflection.

$$\mathtt{I}_{\mathrm{A}[3]}(\phi) = \sum_{\alpha,\beta=1}^{5} \xi_{\alpha\beta} \sum_{j=1}^{3} \mathcal{D}_{\alpha j} \mathcal{D}^*_{\beta j} \tag{27}$$

where the $\xi_{\alpha\beta}$ coefficients can be used to artificially tune the coherence, or interference capability of the fields given in Eq. (24). For maximum coherence, $\xi_{\alpha\beta} = 1$; otherwise $\xi_{\alpha\alpha} = 1$ and $0 \leq \xi_{\alpha\beta} = \xi_{\beta\alpha} < 1$.

IV. EXPERIMENTAL AND SIMULATED RESULTS

The most simple experiment to prove that *Aufhellung*, as considered in Eq. (8), is necessary for describing the *3*-BD process would be by eliminating from $\mathbf{D}_3(\phi)$, Eq. (7), the contributions of all ϕ-dependent *Umweg* channels. Then, a symmetric dip owing to *Aufhellung* should be observed in the ϕ-scan. In fact, the linear polarization of

the synchrotron radiation can be used to eliminate simultaneously the contributions from the B+C and B+$\bar{\text{B}}$+A channels. By setting the secondary reflection forbidden by polarization ($\boldsymbol{v}_{\text{B}} \approx 0 \Rightarrow \boldsymbol{D}_{\text{BC}} \approx \boldsymbol{D}_{\text{B}\bar{\text{B}}\text{A}} \approx 0$), the only ϕ-dependent features in $\text{I}_{\text{A}[3]}(\phi)$ are provided by *Aufhellung*, $b \neq 0$, besides the contribution from the A+$\bar{\text{A}}$+C channel ($\boldsymbol{D}_{\text{A}\bar{\text{C}}\text{C}} \neq 0$).

APPENDIX A

1. Polarization factors

For a linearly polarized X-ray incident beam, whose polarization direction is given by the unit vector $\hat{\boldsymbol{v}}_0$, the polarization factors are calculated as[16,18]

$$\begin{aligned}
\boldsymbol{v}_A &= \hat{\boldsymbol{k}}_{\text{A}} \times (\hat{\boldsymbol{v}}_0 \times \hat{\boldsymbol{k}}_{\text{A}}) & \boldsymbol{v}_B &= \hat{\boldsymbol{k}}_{\text{B}} \times (\hat{\boldsymbol{v}}_0 \times \hat{\boldsymbol{k}}_{\text{B}}) \\
\boldsymbol{v}_{BC} &= \hat{\boldsymbol{k}}_{\text{A}} \times (\boldsymbol{v}_B \times \hat{\boldsymbol{k}}_{\text{A}}) & \boldsymbol{v}_{AA} &= \hat{\boldsymbol{k}}_0 \times (\boldsymbol{v}_A \times \hat{\boldsymbol{k}}_0) \\
\boldsymbol{v}_{AAA} &= \hat{\boldsymbol{k}}_{\text{A}} \times (\boldsymbol{v}_{AA} \times \hat{\boldsymbol{k}}_{\text{A}}) & \boldsymbol{v}_{BB} &= \hat{\boldsymbol{k}}_0 \times (\boldsymbol{v}_B \times \hat{\boldsymbol{k}}_0) \\
\boldsymbol{v}_{BBA} &= \hat{\boldsymbol{k}}_{\text{A}} \times (\boldsymbol{v}_{BB} \times \hat{\boldsymbol{k}}_{\text{A}}) & \boldsymbol{v}_{AC} &= \hat{\boldsymbol{k}}_{\text{B}} \times (\boldsymbol{v}_A \times \hat{\boldsymbol{k}}_{\text{B}}) \\
\boldsymbol{v}_{ACC} &= \hat{\boldsymbol{k}}_{\text{A}} \times (\boldsymbol{v}_{AC} \times \hat{\boldsymbol{k}}_{\text{A}}).
\end{aligned}$$

$\hat{\boldsymbol{k}}_{\text{G}} = \lambda \boldsymbol{k}_{\text{G}}$ is the unit vector along the propagation direction of the beam G. In Eq. (24), all $\hat{\boldsymbol{v}} = \boldsymbol{v}/|\boldsymbol{v}|$.

Knowledge on the values of the Bragg angle θ_X, of reflection X = A, B, and C, provides

$$\begin{aligned}
\hat{\boldsymbol{k}}_0 &= [0,\ 0,\ 1] \\
\hat{\boldsymbol{k}}_{\text{A}} &= [\sin 2\theta_{\text{A}},\ 0,\ \cos 2\theta_{\text{A}}] \\
\hat{\boldsymbol{k}}_{\text{B}} &= [x,\ y,\ \cos 2\theta_{\text{B}}]
\end{aligned}$$

where

$$x = \frac{\cos 2\theta_B - \cos 2\theta_A \cos 2\theta_B}{\sin 2\theta_A}$$

and

$$y = \pm\sqrt{\sin^2 2\theta_B - x^2}.$$

In the used system of reference, the polarization direction of the incident radiation is written as

$$\hat{\boldsymbol{v}}_0 = [-\cos\chi,\ \sin\chi,\ 0].$$

The minus signal is owing to the rotation sense of the diffractometer's χ-axis.

ACKNOWLEDGMENTS

This work was supported by the Brazilian founding agencies FAPESP, grant number 02/10387-5, and CNPq, proc. number 301617/95-3.

* Electronic address: morelhao@if.usp.br

[1] E. Wagner, Phys. Z. **21**, 94 (1932).
[2] S.L. Chang, *Multiple Diffraction of X-Rays in Crystals.* New York: Springer Verlag (1984).
[3] R. Colella, Commun. Condens. Matter Phys. **17**, 175 (1995).
[4] E. Weckert and K. Hümmer, Acta Cryst. A**53**, 108 (1997).
[5] S.L. Chang, Acta Cryst. A**54**, 886 (1998).
[6] H.J. Juretschke, Phys. Rev. Lett. **48**, 1487 (1982).
[7] R. Hoier and K. Marthinsen, Acta Cryst. A **39**, 854 (1983).
[8] Q. Shen Acta Cryst. A**42**, 525 (1986).
[9] K. Hummer and H. Billy, Acta Cryst. A **42**, 127 (1986).
[10] S.L. Chang and M.T. Tang, Acta Cryst. A **44**, 1065 (1988).
[11] Q. Shen and K.D. Finkelstein, Phys. Rev. Lett. **65**, 3337 (1990).
[12] Q. Shen and X.R. Huang, Phys. Rev. B, **63**, 174102 (2001).
[13] Yu.P. Stetsko, G.Y. Lin, Y.S. Huang, C.H. Chao, and S.L. Chang, Phys. Rev. Lett. **86**, 2026 (2001a).
[14] Yu.P. Stetsko, H.J. Juretschke, Y.S. Huang, Y.R. Lee, T.C. Lin, and S.L. Chang, Acta Cryst. A **57**, 359 (2001).
[15] G. Thorkildsen, H.B. Larsen, and E. Weckert, Acta Cryst. A **57**, 389 (2001).
[16] G. Thorkildsen and H.B. Larsen, Acta Cryst. A **58**, 252 (2002).
[17] K. Okitsu, Acta Cryst. A **59**, 235 (2003).
[18] Yu.P. Stetsko, Y.R. Lee, M.T. Tang, and S.L. Chang, Acta Cryst. A **60**, 64 (2004).
[19] G. Thorkildsen, H.B. Larsen, E. Weckert, and D. Semmingsen, Acta Cryst. A **36**, 1324 (2003).
[20] S.L. Morelhão and L.H. Avanci, Acta Cryst. (submitted, available @ http://arxiv.org/abs/cond-mat/0411506).
[21] R. Loudon, *The Quantum Theory of Light.* 3rd ed. Oxford University Press (2000).
[22] M. Renninger, Z. Kristallogr. **97**, 107 (1937).
[23] Q. Shen, S. Kycia, and I. Dobrianov, Acta Cryst. A **56**, 268 (2000).
[24] S.L. Morelhão and S. Kycia, Phys. Rev. Lett. **89**(1), 015501 (2002).
[25] S.L. Morelhão, Acta Cryst. A **59**, 470 (2003).
[26] N. Kato, Acta Cryst. A **32**, 453 (1976).
[27] M. Wormington, C. Panaccione, K.M. Matney, and D.K. Bowen, Phil. Trans. R. Soc. Lond. A **357**, 2827 (1999).
[28] S.L. Morelhão, J. Synchrotron Rad. **10**, 236 (2003).
[29] P.P. Ewald, Ann. Physik (Leipzig) **54**, 519 (1917)
[30] A. Authier, Acta Cryst. A**42**, 414 (1986).
[31] A. Authier and C. Malgrange, Acta Cryst. A**54**, 806 (1998).